Self-Assembly of DNA–Peptide Supermolecules

Coiled-Coil Peptide Structures Templated by d-DNA and l-DNA Triplexes Exhibit Chirality-Independent but Orientation-Dependent Stabilizing Cooperativity

Lou, Chenguang; Boesen, Josephine Tuborg; Christensen, Niels Johan; Sørensen, Kasper K.; Thulstrup, Peter W.; Pedersen, Martin Nors; Giralt, Ernest; Jensen, Knud J.; Wengel, Jesper

Published in:
Chemistry - A European Journal

DOI:
10.1002/chem.201905636

Publication date:
2020

Document version:
Accepted manuscript

Citation for pulished version (APA):
Lou, C., Boesen, J. T., Christensen, N. J., Sørensen, K. K., Thulstrup, P. W., Pedersen, M. N., Giralt, E., Jensen, K. J., & Wengel, J. (2020). Self-Assembly of DNA–Peptide Supermolecules: Coiled-Coil Peptide Structures Templated by d-DNA and l-DNA Triplexes Exhibit Chirality-Independent but Orientation-Dependent Stabilizing Cooperativity. *Chemistry - A European Journal*, *26*(25), 5676-5684. https://doi.org/10.1002/chem.201905636

CHEMISTRY
A European Journal

A Journal of
ChemPubSoc Europe

Accepted Article

Title: Self-assembly of DNA-peptide supermolecules: Coiled-coil peptide structures templated by D-DNA and L-DNA triplexes exhibit chirality-independent but orientation-dependent stabilizing cooperativity

Authors: Chenguang Lou, Josephine Tuborg Boesen, Niels Johan Christensen, Kasper K. Sørensen, Peter Waaben Thulstrup, Martin Nors Pedersen, Ernest Giralt, Knud Jørgen Jensen, and Jesper Wengel

To be cited as: *Chem. Eur. J.* 10.1002/chem.201905636

Link to VoR: http://dx.doi.org/10.1002/chem.201905636

Supported by
ACES

WILEY-VCH

10.1002/chem.201905636

WILEY-VCH

Self-assembly of DNA-peptide Supermolecules: Coiled-coil Peptide Structures Templated by D-DNA and L-DNA Triplexes Exhibit Chirality-independent but Orientation-dependent Stabilizing Cooperativity

Chenguang Lou[+],[a] Josephine Tuborg Boesen[+],[b] Niels Johan Christensen,[b] Kasper K. Sørensen,[b] Peter W. Thulstrup,[c] Martin Nors Pedersen,[d] Ernest Giralt,[e, f] Knud J. Jensen,*[b] and Jesper Wengel*[a]

[a] Dr. C. Lou,[+] Prof. J. Wengel
Biomolecular Nanoscale Engineering Center
Department of Physics, Chemistry and Pharmacy
University of Southern Denmark
Campusvej 55, 5230 Odense M, Denmark
E-mail: jwe@sdu.dk

[b] J. T. Boesen,[+] Dr. N. J. Christensen, Dr. K. K. Sørensen, Prof. K. J. Jensen
Biomolecular Nanoscale Engineering Center
Department of Chemistry
University of Copenhagen
Thorvaldsensvej 40, 1871 Frederiksberg, Denmark
E-mail: kjj@@chem.ku.dk

[c] Prof. P. W. Thulstrup
Department of Chemistry
University of Copenhagen
Universitetsparken 5, 2100 Copenhagen Ø, Denmark

[d] Dr. M. N. Pedersen
X-ray and Neutron Science
Niels Bohr Institute
University of Copenhagen
Universitetsparken 5, 2100 Copenhagen Ø, Denmark

[e] Prof. E. Giralt
Institute for Research in Biomedicine (IRB Barcelona)
Barcelona Institute of Science and Technology (BIST)
Baldiri Reixac 10, Barcelona 08028, Spain

[f] Prof. E. Giralt
Department of Inorganic and Organic Chemistry
University of Barcelona
Martí i Franquès 1-11, Barcelona 08028, Spain

[+] These authors contributed equally to this work

Supporting information and the ORCID identification number(s) for the author(s) of this article can be found under: https://doi.org/10.1002/chem.……

Abstract: DNA nanostructures have been designed and used in many different applications. However, the use of nucleic acid scaffolds to promote the self-assembly of artificial protein mimics is only starting to emerge. Herein five coiled-coil peptide structures were templated by the hybridization of a D-DNA triplex or its mirror-image counterpart, an L-DNA triplex. The self-assembly of the desired trimeric structures in solution was confirmed by gel electrophoresis and small-angle X-ray scattering, and the stabilizing synergy between the two domains was found to be chirality-independent but orientation-dependent. This is the first example of using a nucleic acid scaffold of L-DNA to template the formation of artificial protein mimics. The results may advance the emerging POC-based nanotechnology field by adding two extra dimensions, i.e. chirality and polarity, to provide innovative molecular tools for rational design and bottom-up construction of artificial protein mimics, programmable materials and responsive nanodevices.

Introduction

The programmed self-assembly of oligonucleotides (ONs) through hydrogen bond and π-stacking interactions has inspired the burgeoning development of elaborate two- and three-dimensional DNA nanostructures during the last decades.[1-7] With sizes ranging from nano- to micrometers, the user-defined geometry and the facile chemical functionalization of DNA nanostructures offer ideal nanoscale molecular construction tools for peptide and protein engineering with unparalleled spatial accuracy down to the ångström-scale level with various chemical and biological applications as long term goals.[8-34] However, only a few examples have demonstrated bottom-up construction of artificial protein mimics using the programmability and adaptability of nucleic acid secondary structures, including DNA triplexes,[22,25] G-quadruplexes[14] and multiple DNA junctions.[18,19] The α-helical coiled-coil peptide domains are abundantly found in nature and play

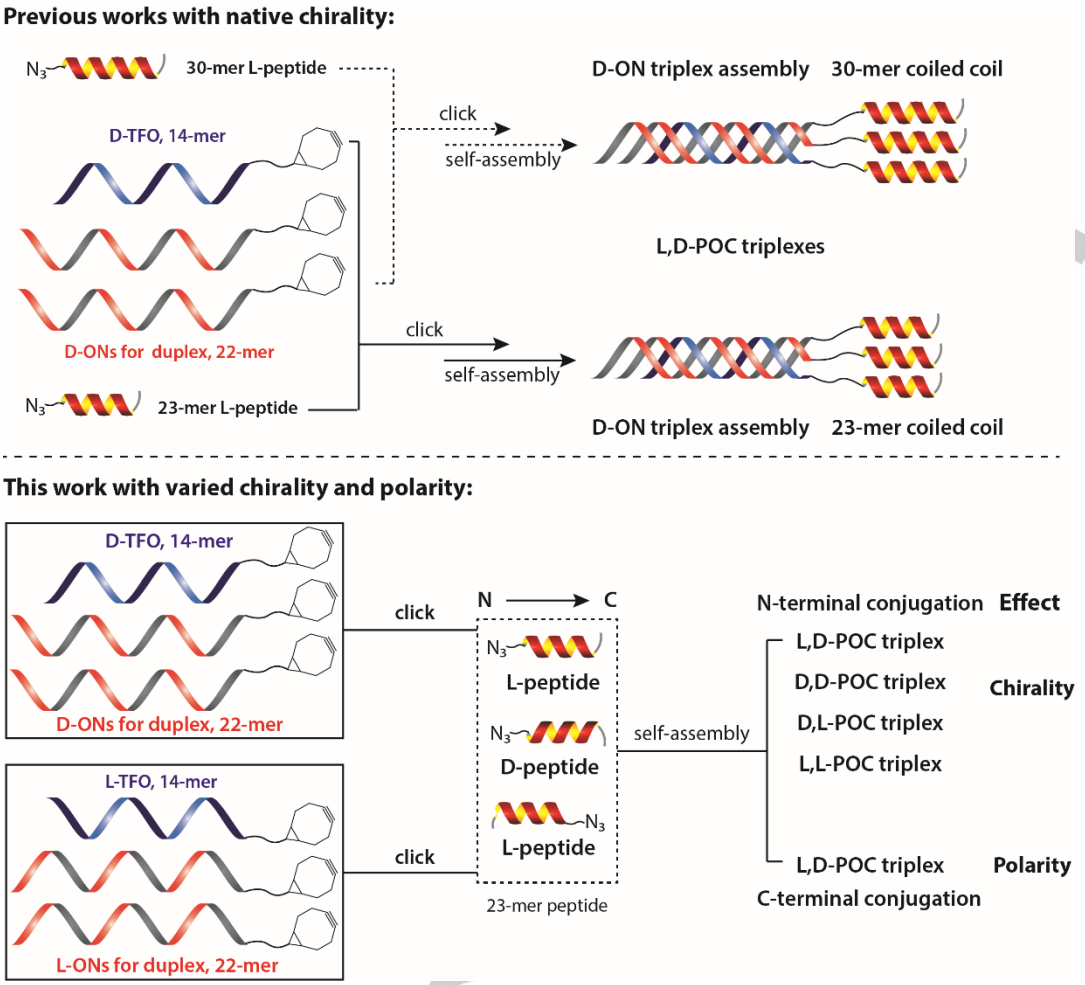

Figure 1. Previous works: *de novo* protein design of peptide coiled-coil structures templated by an ON triplex. **Present study**: It is studied how chirality and polarity of the peptide and ON domains influences the thermostability and structure of the resulting POC triplexes. Key: A two-letter prefix before the POC triplex is used in which the first letter indicates the chirality of the peptide and the second letter the chirality of the ON.

pivotal roles in proteins to mediate various biological processes.[35-40] In the self-repeating heptad sequence (abcdefg), two or more α-helical peptide strands wind around each other in a left- or right-handed conformation via hydrophobic, electrostatic, and hydrogen-bond interactions to generate structures with different topologies and morphologies.[41].

As a proof-of-concept, we have recently reported the self-assembly of peptide-oligonucleotide conjugates (POCs), where the peptides form trimeric coiled-coil bundles, while the ONs form a triple helix. A 30-mer peptide sequence was conjugated to each of three ONs capable of hybridization to form a triplex nucleic acid scaffold (Figure 1, previous work).[22] In a first step to dissect the self-assembly process of such POC-based complexes, we truncated the peptide from a 30-mer to a 23-mer sequence and observed that the POC was still able to self-assemble into a monodisperse trimeric peptide bundle, with the formation of an ON triplex as driving force (Figure 1, previous work).[25]

It remains important to understand the cooperativity of the self-assembly process and elucidate the factors which play roles in this process. For example, is the folding of one of the bio-oligomers influenced by the change in the physical attributes of the other? Herein we have systematically varied the chirality of the peptide and the ON, as well as the orientation of POCs, i.e. whether the DNA is anchored to the N- or C-terminus of the peptide (Figure 1, this work). We have studied whether the chirality of the ON triplex scaffold and the coiled-coil peptide bundle, as well as polarity inversion of the coiled-coil peptide bundle, affects the structure of the POC-based self-assemblies. To achieve this aim we synthesized the 23-mer peptide as both the L- and D-enantiomers (N-terminal azide), as well as the 23-mer L-peptide sequence with an additional ε-azido-lysine at the C-terminus, derived from coil-V_aL_d[42] with an additional azidohexanoyl-Tyr residue. The 23-mer L-peptide[43] and its mirror-image sequence were synthesized from L-amino acids and D-amino acids, respectively. Reversing the directionality of the peptide bundle was realized by moving the azido function from the N-terminus to the C-terminus of the peptide sequence using an azidolysine attached to the carboxylate of the terminal glycine residue. This maneuver is almost perfect, with no additional bond being introduced into the interdomain linker. The helical wheel representations (Figure S1) show how the three 23-mer peptides associate into coiled-coil domains and indicate the location of azide handles for N- and C-terminal conjugation. Conjugation of these three peptides to each strand of the D-ON triplex scaffold through copper-free azido-alkyne cycloaddition reactions provided in total nine POCs as the building blocks for

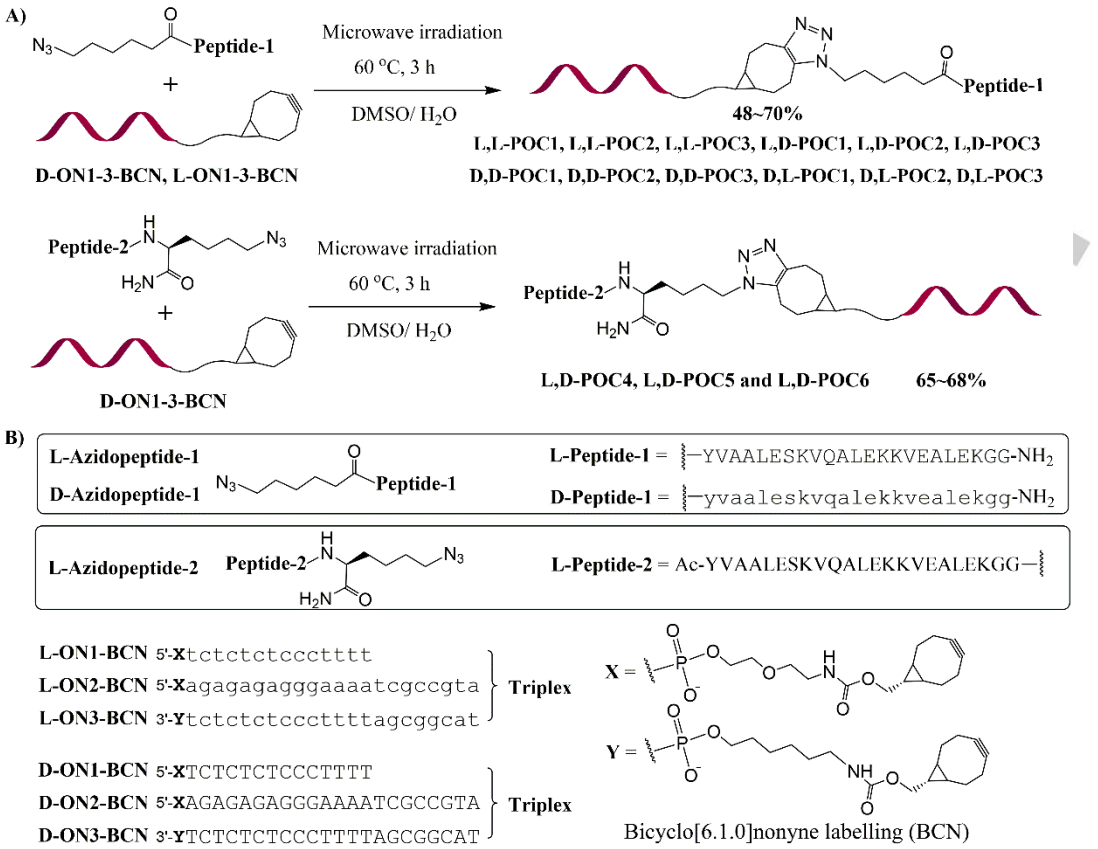

Figure 2. Synthesis of 15 peptide-ON conjugates (POCs). A) The click chemistry between azidopeptides and BCN-functionalized ONs. B) Sequence of **L-azidopeptide-1**, **D-azidopeptide-1**, **L-azidopeptide-2** and **L-ON1-BCN**, **L-ON2-BCN**, **L-ON3-BCN**, **D-ON1-BCN**, **D-ON2-BCN** and **D-ON3-BCN**. The reaction yields are given as a range, and the actual yield for each POC can be found in Figure S7 and S14. D and L represent the chirality of the amino acids and nucleotides used to construct the peptides or ONs and thus also the overall chirality of the peptides or ONs. Natural nucleosides and amino acids are denoted in upper cases while unnatural ones are in lower cases. Thus, A, G, C and T are D-DNA monomers while a, g, c, t are L-DNA monomers. Y, V, L, E, S, K, Q, A, G are L-amino acids whereas y, v, l, e, s, k, q, a, g are D-amino acids. Key: The two-letter prefix before POC1, POC2, POC3, POC4, POC5 and POC6: The first letter indicates the chirality of the peptide while the second letter indicates the chirality of the ON.

the self-assembly of three artificial protein mimics. As the mirror-image counterpart of natural D-DNA, L-DNA possesses an inherent resistance towards nucleolytic degradation and generally low immunogenicity.[44,45] Thus, L-DNA has certain advantages over its natural counterpart as nucleic acid scaffolds for biological applications. Herein, L-DNA was applied for the first time to serve as the nucleic acid scaffold in a left-handed ON triplex, to template the formation of an artificial three-helix protein mimic based on a 23-mer L-peptide. Also, the mirror-image peptide bundle derived from the corresponding D-peptide was assembled based on the L-DNA triple helix as template. This required additional six POCs as building blocks.

Results and Discussion

POC synthesis

We relied on our previous POC synthesis strategy,[25] such that the bioconjugations between bicyclo[6.1.0]nonyne (BCN)-functionalized ONs and azide-modified peptides were accomplished via copper-free ring-strain promoted azide-alkyne cycloaddition (Figure 2). All involved ONs were synthesized from commercially available D-nucleoside or mirror-image L-nucleoside monomers via phosphoramidite chemistry and standard automated DNA synthesis. Due to the lack of commercially available inverted L-nucleoside phosphoramidite monomers, the BCN functionalization of **D-ON**s and **L-ON**s was realized in a two-step procedure, 1) a primary amine linker which was first incorporated at either the 5'-end or the 3'-end of ONs during automated nucleic acid synthesis (Figure S3); 2) the alkyne function was subsequently introduced through NHS ester chemistry in liquid-phase so-called post-ON synthesis (Scheme S1, Figure S4 and Figure S5). Only **L-ON2-BCN** and **L-ON3-BCN** were synthesized as previously described (Figure S6).[22,25] On the other hand, the corresponding azide handle was introduced via solid-phase peptide synthesis either as azidohexanoyl-Tyr on the N-terminus of the peptides (**L-azidopeptide-1** derived from L-amino acids and **D-azidopeptide-1** from D-amino acids) or as ε-azido-lysine on the C-terminus of the peptide (**L-azidopeptide-2**) (Figure 2b and Figure S2). Azide-alkyne coupling reactions between BCN-functionalized ONs and azide-modified peptides were carried out under microwave heating condition, whereby fifteen POCs were obtained in an efficient and high-yielding manner (Figure 1 and Figures S7-S16 in ESI).

Ultraviolet thermal denaturation and gel electrophoresis studies

Table 1. UV-melting studies.[a]

Entry	Duplex/triplex	Melting	Annealing	Structure
D-DNA series				
1	**D-(ON1+ON2+ON3)**	35.0 ± 0.1 °C (63.7 ± 0.3 °C)	33.4 ± 0.1 °C (63.7 ± 0.4 °C)	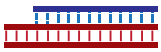
2	**L,D-(POC1+POC2+POC3)**	53.5 ± 0.2 °C (64.7 ± 0.1 °C)	54.0 ± 0.3 °C (64.6 ± 0.5 °C)	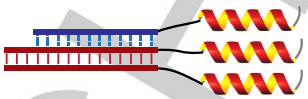
3	**D,D-(POC1+POC2+POC3)**	53.6 ± 0.2 °C (66.5 ± 0.3 °C)	53.3 ± 0.1 °C (66.5 ± 0.4 °C)	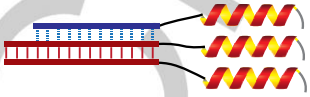
4	**L,D-(POC4+POC5+POC6)**	48.9 ± 0.1 °C (66.1 ± 0.2 °C)	48.4 ± 0.2 °C (65.7 ± 0.1 °C)	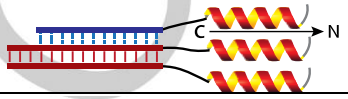
L-DNA series				
5	**L-(ON1+ON2+ON3)**	35.4 ± 0.1 °C (64.1 ± 0.3 °C)	33.7 ± 0.1 °C (64.0 ± 0.1 °C)	
6	**L,L-(POC1+POC2+POC3)**	54.0 ± 0.6 °C (65.0 ± 0.1 °C)	53.6 ± 0.3 °C (65.1 ± 0.1 °C)	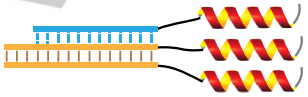
7	**D,L-(POC1+POC2+POC3)**	54.3 ± 0.2 °C (65.9 ± 0.1 °C)	54.0 ± 0.1 °C (65.9 ± 0.2 °C)	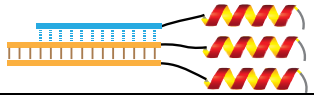

[a] Thermal denaturation and annealing temperatures (T_m and T_a values) of POC and ON-reference triple helixes measured at pH 5.5 as an average of three independent melting temperature determinations shown with the corresponding standard deviations. The values in brackets are T_m and T_a values measured for the corresponding underlying duplexes. The experiments were recorded at 275 nm in 10 mM acetate buffer (NaOAc/HOAc) containing 100 mM NaCl. The concentration of the individual duplex components was 1.0 µM while the TFO component was used in 1.5 µM concentration. The peptide moiety is marked in yellow and red (L-peptide as right-handed helix, D-peptide as left-handed helix), the TFO moiety in dark blue (D-nucleotide) or light blue (L-nucleotide), and the DNA duplex moiety in crimson (D-nucleotide) or in orange (L-nucleotide).

With 15 POCs and the corresponding ON controls in hand, the thermal stability of the triplex scaffold was evaluated for five assemblies where peptides formed a parallel coiled-coil domain. Templated by D-ON triplex formation, two mirror-image coiled-coil trimers were self-assembled from two stereoisomeric 23-mer peptides (L-peptide-1 and D-peptide-1), respectively. Therefore, one aim was to investigate whether the chirality change on the peptide domain could influence the thermal stability of the triple helical assemblies. Additionally, an unnatural L-DNA triplex, mirrored from the D-DNA triplex template, was used as an innately nuclease-resistant scaffold[45] to template the formation of those two mirror-image coiled-coil trimeric structures. Furthermore, possible orientation-dependent effects, such as dipole moment and hydrogen bonds, were evaluated through inverting the polarity of the peptide by moving the conjugation point from the N-terminus to the C-terminus of the peptide sequence. This was achieved by introduction of an additional C-terminal ε-azido-lysine. In accord with our previous reports,[22,25] 275 nm was chosen to record the ultraviolet absorbance as the function of temperature, at which wavelength the peptide units and coiled-coil structures showed negligible absorption (See Figures S17-S19).

When natural D-nucleotides were utilized to constitute the triplex scaffold, compared to **D-(ON1+ON2+ON3)**, both **L,D-(POC1+POC2+POC3)** and **D,D-(POC1+POC2+POC3)** showed substantially increased triplex stability (Table 1, entries 1-3), clearly reflecting the strong stabilizing cooperativity between the ON triplex domain and the trimeric peptide bundle. There was no noticeable change in triplex melting temperature whether the L-peptide coiled-coil or its mirror-image was assembled. This indicates that the chirality of the peptide trimer has no significant influence on the thermodynamic stability of the D-ON triplex, which was further substantiated using the L-ON triplex to template the formation of two mirror-image coiled-coil structures (Table 1, entries 6 and 7). Interestingly, when the D-ON triplex template was moved from the N-termini to the C-termini of the trimeric peptide bundle, a minor decrease in the triplex melting temperature was observed. Possible causes for this destabilizing effect are (i) the flipped dipole moment of the coiled coil, and (ii) a minute change of the local chemical environment at the ON-peptide junction due to different amino acids. Moreover, relative to **D-(ON1+ON2+ON3)**, a strong triplex stabilizing effect was well preserved in the case of **L,D-(POC4+POC5+POC6)** (Table 1, entry 4), which confirmed the cooperative stabilization between the ON and peptide domains. Triplex denaturation studies were also carried out on all hybrid triple helical structures with a varying number of peptide strands attached. The results again demonstrated the ability of the triple-stranded peptide bundle to deliver stabilizing cooperativity (See Table S1-S5 in ESI).

The annealing thermodynamic profile of all the triple helical structures validates the trends concluded from triplex melting studies (See Table S1-S5). In contrast to our previous POCs,[22,25] all hybrid triplexes exhibited clear triplex annealing

transitions probably owing to the accelerated kinetics under pH 5.5 used in the current study. In addition, upon the dissociation of the third strand, the underlying duplexes in the five assemblies exhibited a marginal increase in duplex melting temperature compared to the respective controls, likely due to the presence of two parallel peptide strands. A similar tendency was also observed in duplex denaturation studies (See Table S1-S5).

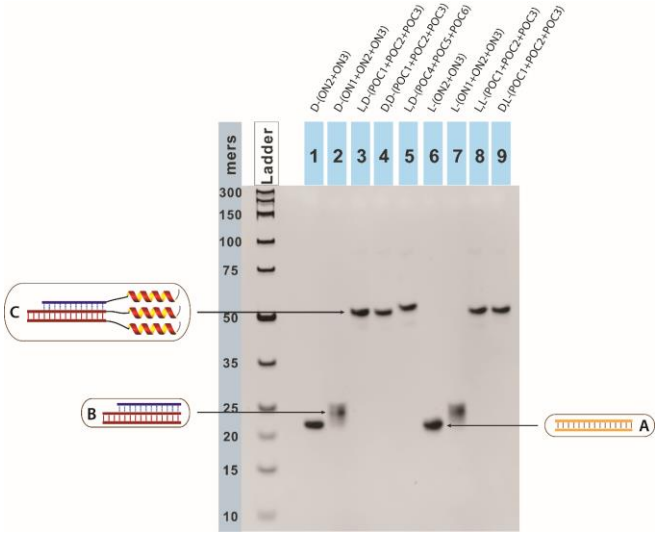

Figure 3. Non-denaturing 13% PAGE at pH 5.5 and 4 ˚C. The gel was visualized by ultraviolet excitation at 260 nm after ethidium bromide staining. The O'GeneRuler Ultra Low Range DNA Ladder from bottom to top: 10, 15, 20, 25, 35, 50, 75, 100, 150, 200 and 300 mers. The peptide moiety is marked in alternating yellow and red, the D-ON TFO moiety is in blue, the D-ON duplex is in crimson and the L-ON duplex is in light orange.

The five POC triplex assemblies, as well as the ON duplex and triplex controls, were characterized by non-denaturing polyacrylamide gel electrophoresis (native PAGE) at 4 ˚C and a relatively low voltage. These mild experimental conditions were chosen to minimize possible dissociation of the triple helical structures. As expected, **D-(ON2+ON3)** and **L-(ON2+ON3)** had a higher gel mobility, with their bands located close to the 20-mer DNA marker (Figure 3, lane 1 and 6). Upon binding of the third strands (**D-ON1** or **L-ON1**) to the major groove of these two duplexes, the resulting **D-(ON1+ON2+ON3)** and **L-(ON1+ON2+ON3)** showed slightly reduced in-gel mobility, providing two major bands at level with the 25-mer DNA marker (Figure 3, lane 2 and 7). A smearing region in front of each may be caused by the minor dissociation of **D-ON1**/**L-ON1** from the triplex helixes. When the ON triplex was formed by three POCs having trimeric peptide coiled-coil structure of different chirality or polarity (Figure 3, lane 3, 4, 5, 8 and 9), a single band was uniformly observed, indicating the monodisperse state of each assembled trimeric complex in solution, at least under the experiment condition employed. Relative to the ON triplex controls, significant retardation in gel mobility was noted, which can be attributed to the higher mass-charge ratio and increased molecular size.

Circular dichroism thermal denaturation studies

A series of UV circular dichroism (CD) spectroscopic experiments were conducted and are plotted as the relative ellipticity at 220 nm in Figure 4 and given in Table S7 and S8. **D-(ON1+ON2+ON3)** and **L-(ON1+ON2+ON3)** exhibited a clear triplex melting transition (Figure 4, Table S7), whereas no further transition was observed for the unfolding of the underlying duplexes **D-(ON2+ON3)** and **L-(ON2+ON3)**. The given triplex melting temperature was congruent with the data obtained in UV thermal denaturation results (entry 1 and 2, Table S7), and the transition disappeared at higher pH (pH 6.0, Figure S33). The CD signal of the two ON triplexes have a sign inversion with a zero-crossing at approximately 40 °C with the signals merging around zero again at 90 °C. No obvious melting transition was observed for the unconjugated peptide controls as these are not folded to any significant extent as free peptides (Figure 4), although the C-terminally modified peptide did display slightly more CD intensity at lower temperatures. All enantiomeric pairs of samples display mirror-image symmetry in their thermal unfolding behaviour. The largest CD signal intensities are observed for the **D,L-(POC1+POC2+POC3)** and **L,D-(POC1+POC2+POC3)** pair that have the same signed contributions from both peptide and ON components in the POC triplex forms. Interestingly, in the folded state (20-30 °C) the intensity difference between e.g. **D,L-(POC1+POC2+POC3)** and **D,D-(POC1+POC2+POC3)** was larger than the difference between **L-(ON1+ON2+ON3)** and **D-(ON1+ON2+ON3)**. This indicates that there could be a difference in folding between these diastereomeric forms. As denaturing sets in, the curves cross each other due to the sign change of the ON contribution. All POC-based triple-helical ensembles give sigmoidal or near-sigmoidal curves, the melting process is assumed to be the outcome of cooperative dissociation of the ON triplex and the coiled coil trimer structure and it is not trivial to deconvolute the composite signals. Thus, the dissociation of TFO from the ON triple helix is overlaid with the melting of the trimeric coiled-coil. Unfortunately, we were unable to isolate the melting transition of the coiled coil domain from these two highly cooperative dissociation events.

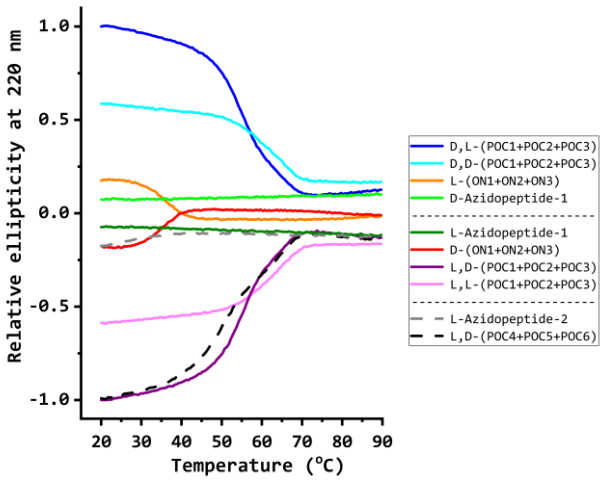

Figure 4. UV Circular Dichroism melting studies of POCs, ONs and peptides. 10 mM acetate buffer, 100 mM NaCl, pH 5.5. Measured at 220 nm at 0.5 ˚C intervals between 20 ˚C and 90 ˚C. Concentration (9 μM) for all samples as determined by UV absorbance at 260 nm. Intensities have been normalized with respect to the samples with the maximum intensity. See the keys in **Figure 2**.

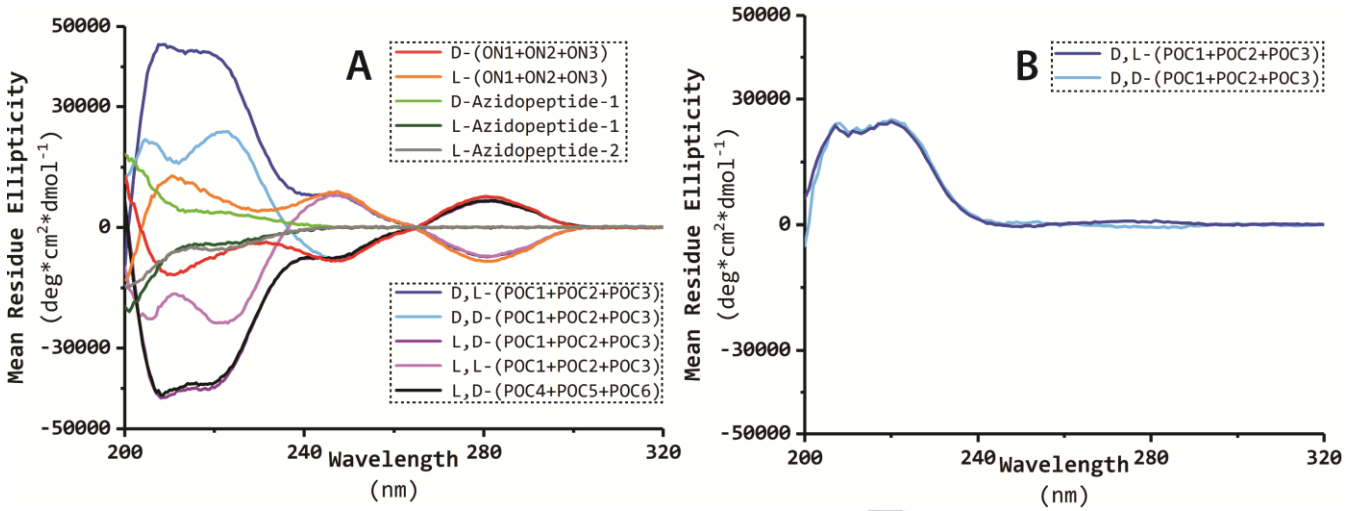

Figure 5. A. Circular dichroism spectra in 10 mM acetate buffer, 100 mM NaCl pH 5.5, from 320-200 nm. All samples are 9 μM as determined by UV absorbance at 260 nm. **B.** Isolated peptide spectra of **D,L-(POC1+POC2+POC3)** 13.2 μM and **D,D-(POC1+POC2+POC3)** 10.6 μM. Spectra of ONs have been subtracted from spectra of POCs. Corrected for concentration based on concentrations found from amino acid analysis (AAA).

In contrast, when the conjugation point was moved from the N-terminus to the C-terminus of the coiled-coil structure, **L,D-(POC4+POC5+POC6)** gave a biphasic-like melting transition, where the melting temperature derived from the first transition is very close to the TFO dissociation temperature recorded for the ON triplex scaffold in the UV thermal denaturation studies (entry 5, Table S7). Furthermore, the amplitude of the first melting transition is substantially larger than of the control **D-(ON1+ON2+ON3)**, indicating that the dissociation of TFO from the ON duplex presumably was accompanied by the separation of its conjugated peptide from the other two peptides connected to the ON duplex scaffold. Relative to **L,D-(POC1+POC2+POC3)**, **L,D-(POC4+POC5+POC6)** however showed a significant decrease in the triplex melting temperature (entry 4 vs entry 5, Table S7), which is interpreted as the cooperative dissociation events of both the TFO and its conjugated peptide, reflecting that the stability of POC triple helix is strongly dependent on the orientation of the templated coiled-coil trimer. This interpretation was further substantiated by increasing the pH to 6.0 (entry 6 and 7, Table S7); Thus, if the first melting transition indeed derived from the dissociation of the third strand, higher pH would lead to lowering of the melting temperature due to the reduced binding affinity of the TFO towards the ON duplex.[46,47] Gratifyingly, a decrease in the melting temperature by 17.3˚C was observed when the pH was increased from 5.5 to 6.0 (entry 5 and 7 in Table S7, Figure S33), which nicely matches the results obtained from UV-melting studies (ΔT_m = 16.3˚C, entry 5 and 7 in Table S7). Besides, a melting temperature at lower range (55.2˚C) was recorded for **L,D-(POC1+POC2+POC3)** at pH 5.5, which agrees well with that of the TFO dissociation temperature in UV-melting studies (53.5˚C). The same consistency was observed for **D,L-(POC1+POC2+POC3)** and **L,D-(POC4+POC5+POC6)** at pH 5.5, as well as **L,D-(POC1+POC2+POC3)** and **L,D-(POC4+POC5+POC6)** at pH 6.0. From them, an interesting trend was noticed, namely that the dissociation temperatures of the TFO-containing POC derived from the CD melting at 220 nm, thus primarily from the α-helical peptides, were always slightly higher than those extracted from UV thermal denaturation on the ON triplex scaffolds at 260 nm (entry 3-7 in Table S7). This indicates that the melting processes could initiate from the non-conjugated side of the TFO-containing POC. The second melting transition is regarded as the dissociation of the two peptide strands linked to the underlying ON duplex, of which the melting temperatures were found to be markedly lower than those from UV-melting studies (the bracket values in entry 5-7, Table S7). This may imply that the de-coiling of the remaining two-helix peptide bundle precedes the decomposition of the ON duplex scaffold.

Circular dichroism spectroscopic studies

CD spectra were recorded to investigate how the α-helicity from the coiled-coil structure could be influenced by the chirality change in the ON triplex scaffold, and by the inverted orientation by moving the ON triplex template from the N-terminus to the C-terminus (Figure 5A). In general, two mirror-imaged ensembles gave a pair of ellipticity curves with near-perfect symmetry along the zero baseline, including **L-azidopeptide-1** and **D-azidopeptide-1**, **L-(ON1+ON2+ON3)** and **D-(ON1+ON2+ON3)**, **D,L-(POC1+POC2+POC3)** and **L,D-(POC1+POC2+POC3)**, **D,D-(POC1+POC2+POC3)** and **L,L-(POC1+POC2+POC3)**. The signal recorded for **L-Azidopeptide-2** (with the azide on the C-terminus) is very similar to that of **L-azidopeptide-1**, when taking its 24-mer sequence length into account. It is noted that **L,D-(POC4+POC5+POC6)** showed almost identical α-helicity signal to that of **L,D-(POC1+POC2+POC3)**, which underscores the robustness of the templating effect of the nucleic acid scaffold and the high adaptability between the two domains as long as the ensembles are kept well below their triplex melting temperature. The two ends of the peptide may be dynamically different, but we have now shown that both ends are relatively similar in availability and can be used for conjugation with ONs. The α-helicity signal was overlaid with the ellipticity derived from the ON triplex template, significantly complicating the signal interpretation upon the chirality change in the ON triple helix

(Figure 5A). Thus, it becomes necessary to subtract the contribution of the ON triple helix from the CD spectra to isolate the α-helicity signal solely from the coiled-coil structure to delineate possible influence.

Considering the limited accuracy of using UV absorbance at 260 nm wavelength to determine the concentration of POCs, several representative POC ensembles were quantified by amino acid analysis (AAA) as an orthogonal method for concentration determination (Figure S29). The concentrations determined by the AAA were in general higher than the concentrations determined by UV. This gave a lower degree of α-helicity than that calculated from the 9 μM concentration obtained by UV. Using the concentrations from AAA we obtained near-perfect mirror images of the two CD spectra of **D,L-(POC1+POC2+POC3)** and **L,D-(POC1+POC2+POC3)** (Figure S30). This supports the validity of the concentration determination through AAA. The concentrations of the **D,D-(POC1+POC2+POC3)** sample was slightly higher according to AAA than UV absorbance. In our preceding publications,[22,25] the concentrations of individual POC strands were determined by UV absorbance only. For direct comparison, with the concentrations of the two corresponding ON triplexes determined by UV absorbance, the isolation of the α-helicity signal from the CD spectra of POC-based ensembles was also performed with the concentration determined by UV-absorbance (Figure S31).

Taking **D,D-(POC1+POC2+POC3)** and **D,L-(POC1+POC2+POC3)** as a model system (Figure 5B), isolating the α-helicity signal from their CD spectra were accomplished by subtracting the spectra recorded for the corresponding ON triplexes, **D-(ON1+ON2+ON3)** and **L-(ON1+ON2+ON3)**. It is assumed that no significant conformation change occurs in the ON triplex template of POC-based ensembles. The following can be concluded: 1) Consistent with our previous work, the ON triplex scaffold provided a strong templating effect, inducing an intensive α-helical signal and similar degree of helix association for the coiled-coil structure; 2) the chirality change of the ON triplex template did not exert a strong influence on the cooperative stability of the three peptide strands in the D-peptide coiled-coil structure, which is substantiated by 69.3% vs 67.5% helical contents calculated from θ_{222} for **D,D-(POC1+POC2+POC3)** and **D,L-(POC1+POC2+POC3)**, respectively (Figure 5B and Table S9). Thus, the chirality of the ON triplex did not affect the folding of the peptide bundle (Figure S30). Calculation of helical contents for POC self-assemblies were also performed using the concentrations determined by UV absorbance (Table S9), where a similar tendency was observed but with a larger deviation probably as a result of relatively lower accuracy compared to AAA. To sum up, the chirality change of the ON triplex template has no significant impact on the amplitude of the helical signal, nor the α-helical content, which also nicely echoes the results obtained from UV thermal denaturation. Considering the long incubation time (12 h in fridge) during sample preparation, all results concluded here are assumed to be related to the thermodynamically most stable complexes being formed under the conditions used.

Small-angle X-ray scattering (SAXS) analysis

The size and shape of three POC self-assemblies in solution was examined with small-angle X-ray scattering (SAXS) at POC concentrations of 10 μM and 50 μM (Figure 6 and Supporting Figures S35-S41) to study whether altering the chirality or the orientation of the ON or peptide domains affected the overall shape of the conjugates. **L,D-(POC1+POC2+POC3)** has the same chirality as our previous POC systems, although with a slightly altered ON sequence,[25] while in **L,D-(POC4+POC5+POC6)** the attachment point was moved to the C-terminus. For analyses of the experimental SAXS data, we first performed 100 ns restrained MD simulations on **L,D-(POC1+POC2+POC3)** and **L,D-(POC4+POC5+POC6)** and extracted ~1000 conformations, which were fitted to the experimental data using the FoXS program.[48] A single molecular model with a kink in the linker region (Figure 6) with an obtuse angle between the DNA and peptide domains gave good fits for both systems at 10 μM.

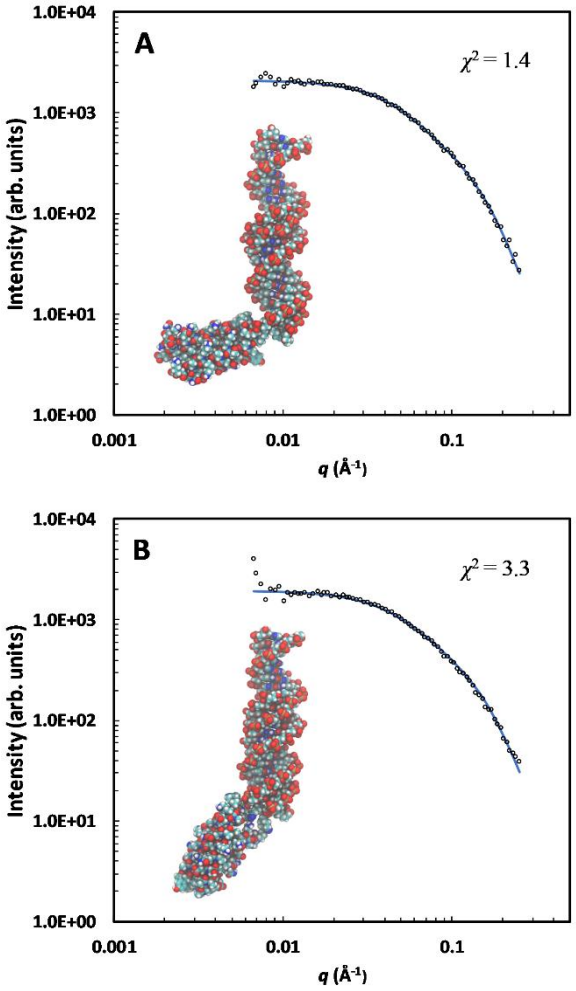

Figure 6. SAXS measurements (10 μM) and predictions from molecular models. **A. L,D-(POC1+POC2+POC3)** and **B. L,D-(POC4+POC5+POC6)**. The goodness of fit is FoXS χ^2.

The SAXS measurements for **D,L-(POC1+POC2+POC3)**, for which the chirality of both peptide and DNA was inverted relative to **L,D-(POC1+POC2+POC3)**, were highly similar to the latter **(**Figure S41). This showed that the POC self-assemblies formed in a robust manner independently of chirality. The small difference in the SAXS structure was likely due to small

variations in experimental conditions. In **L,D-(POC4+POC5+POC6)** the orientation of the peptides was inverted, however, the overall shape was retained, but with a small change to the angle of the kink. Thus, the combination of SAXS and modelling supports that **L,D-(POC1+POC2+POC3)**, **L,D-(POC4+POC5+POC6)**, and **D,L-(POC1+POC2+POC3)** are well-defined molecular assemblies that do not aggregate at 10 µM. Also, SAXS data obtained for 50 µM POC concentrations (Figures S36, S38, S40) do not indicate aggregation and the SAXS curves could be fitted with slightly different conformations of the structures in Figure 6 (not shown).

We therefore conclude that these three different POC self-assemble into stable trimers at µM concentrations and that the overall shape is comparable to our previously studied POCs. This confirms the robustness of this POC design. The POC where the peptides were C-terminally attached gave a slightly altered angle, which could be due to small differences in the packing around the triazole linkage region.

Conclusion

The self-assembly of the POCs occurred by cooperative formation of the coiled-coil peptide structures and the hybridization of ON triplex scaffolds. This happened in a chirality-independent manner but with a small effect while attaching the ON via the peptide C- or N-terminal, respectively, had a small effect on melting temperature, as seen from the melting studies on ON triplex and peptide trimeric coiled-coil (loss of TFO-containing POC). An L-DNA triple helix, composed of mirror image nucleotides relative to the natural nucleotides, was employed for the first time as a molecular scaffold to drive the formation of peptide bundles. These results substantiate how bottom-up construction of protein mimics, using nucleic acid secondary structures as the templates, can be realized. This approach may pave the way for rational design of functional artificial protein mimics for biological and biomedical applications.

Acknowledgements

The VILLUM FONDEN is thanked for funding the Biomolecular Nanoscale Engineering Center (BioNEC), a VILLUM center of excellence, grant number VKR18333. Joan Hansen and Tina Grubbe Hansen are thanked for technical assistance on oligonucleotide synthesis and purification.

Keywords: oligonucleotide triplexes • peptide coiled-coils • peptide-oligonucleotide conjugates • chirality • sequence polarity

[[1] J. Chen, N. C. Seeman, *Nature* **1991**, 350, 631-633.
[2] F. A. Aldaye, A. L. Palmer, H. F. Sleiman, *Science* **2008**, 321, 1795-1799.
[3] H. Yin, R. L. Kanasty, A. A. Eltoukhy, A. J. Vegas, J. R. Dorkin, D. G. Anderson, *Nat. Rev. Genet.* **2014**, 15, 541-555.
[4] N. C. Seeman, H. F. Sleiman, *Nat. Rev. Mater.* **2017**, 3, 17068.
[5] Z. Qing, J. Xu, J. Hu, J. Zheng, L. He, Z. Zou, S. Yang, W. Tan, R. Yang, *Angew. Chem. Int. Ed.* **2019**, 58, 11574-11585.
[6] Q. Q. Hu, H. Li, L. H. Wang, H. Z. Gu, C. H. Fan, *Chem. Rev.* **2019**, 119, 6459-6506.
[7] M. Madsen, K. V. Gothelf, *Chem. Rev.* **2019**, 119, 6384-6458.
[8] H. Li, S. H. Park, J. H. Reif, T. H. LaBean, H. Yan, *J. Am. Chem. Soc.* **2004**, 126, 418-419.
[9] J. Wengel, *Org. Biomol. Chem.* **2004**, 2, 277-280.
[10] S. H. Park, P. Yin, Y. Liu, J. H. Reif, T. H. LaBean, H. Yan, *Nano Lett.* **2005**, 5, 729-733.
[11] O. I. Wilner, Y. Weizmann, R. Gill, O. Lioubashevski, R. Freeman, I. Willner, *Nat. Nanotechnol.* **2009**, 4, 249-254.
[12] B. A. R. Williams, C. W. Diehnelt, P. Belcher, M. Greving, N. W. Woodbury, S. A. Johnston, J. C. Chaput, *J. Am. Chem. Soc.* **2009**, 131, 17233-17241.
[13] H. Eberhard, F. Diezmann, O. Seitz, *Angew. Chem. Int. Ed.* **2011**, 50, 4146-4150.
[14] P. S. Ghosh, A. D. Hamilton, *J. Am. Chem. Soc.* **2012**, 134, 13208-13211.
[15] E. A. Englund, D. Wang, H. Fujigaki, H. Sakai, C. M. Micklitsch, R. Ghirlando, G. Martin-Manso, M. L. Pendrak, D. D. Roberts, S. R. Durell, D. H. Appella, *Nat. Commun.* **2012**, 3, 614.
[16] B. M. G. Janssen, E. H. M. Lempens, L. L. C. Olijve, I. K. Voets, J. L. J. van Dongen, T. F. A. de Greef, M. Merkx, *Chem. Sci.* **2013**, 4, 1442-1450.
[17] S. A. Kazane, J. Y. Axup, C. H. Kim, M. Ciobanu, E. D. Wold, S. Barluenga, B. A. Hutchins, P. G. Schultz, N. Winssinger, V. V. Smider, *J. Am. Chem. Soc.* **2013**, 135, 340-346.
[18] S. I. Liang, J. M. McFarland, D. Rabuka, Z. J. Gartner, *J. Am. Chem. Soc.* **2014**, 136, 10850-10853.
[19] M. Humenik, T. Scheibel, *ACS Nano* **2014**, 8, 1342-1349.
[20] N. Stephanopoulos, R. Freeman, H. A. North, S. Sur, S. J. Jeong, F. Tantakitti, J. A. Kessler, S. I. Stupp, *Nano Lett.* **2015**, 15, 603-609.
[21] M. R. Jones, N. C. Seeman, C. A. Mirkin, *Science* **2015**, 347, 1260901.
[22] C. Lou, M. C. Martos-Maldonado, C. S. Madsen, R. P. Thomsen, S. R. Midtgaard, N. J. Christensen, J. Kjems, P. W. Thulstrup, J. Wengel, K. J. Jensen, *Nat. Commun.* **2016**, 7, 12294.
[23] Q. Luo, C. Hou, Y. Bai, R. Wang, J. Liu, *Chem. Rev.* **2016**, 116, 13571-13632.
[24] A. D. Merg, R. V. Thaner, S. Mokashi-Punekar, S. T. Nguyen, N. L. Rosi, *Chem. Commun.* **2017**, 53, 12221-12224.
[25] C. Lou, N. J. Christensen, M. C. Martos-Maldonado, S. R. Midtgaard, M. Ejlersen, P. W. Thulstrup, K. K. Sørensen, K. J. Jensen, J. Wengel, *Chem. Eur. J.* **2017**, 23, 9297-9305.
[26] C. Guo, R. Hili, Bioconjug. Chem. 2017, 28, 314-318.
[27] A. Chotera, H. Sadihov, R. Cohen-Luria, P.-A. Monnard, G. Ashkenasy, *Chem.: Eur. J.* **2018**, 24, 10128-10135.
[28] K. Astakhova, R. Ray, M. Taskova, J. Uhd, A. Carstens, K. Morris, *Mol. Pharm.* **2018**, 15, 2892-2899.
[29] F. Charbgoo, M. Alibolandi, S. M. Taghdisi, K. Abnous, F. Soltani, M. Ramezani, *Nanomedicine* **2018**, 14, 685-697.
[30] E. Spruijt, S. E. Tusk, H. Bayley, *Nat. Nanotechnol.* **2018**, 13, 739-745.
[31] K. Zhou, Y. Ke, Q. Wang, *J. Am. Chem. Soc.* **2018**, 140, 8074-8077.
[32] T. MacCulloch, A. Buchberger, N. Stephanopoulos, *Org. Biomol. Chem.* **2019**, 17, 1668-1682.
[33] J. Jin, E. G. Baker, C. W. Wood, J. Bath, D. N. Woolfson, A. J. Turberfield, *ACS Nano* **2019**, 13, 9927-9935.
[34] N. Stephanopoulos, *Bioconjug. Chem.* **2019**, 30, 1915-1922.
[35] J. Walshaw, D. N. Woolfson, *J. Mol. Biol.* **2001**, 307, 1427-1450.
[36] P. Burkhard, J. Stetefeld, S. V. Strelkov, *Trends Cell Biol.* **2001**, 11, 82-88.
[37] A. N. Lupas, M. Gruber, in *Advances in Protein Chemistry*, Vol. 70, Academic Press, **2005**, pp. 37-38.
[38] E. Moutevelis, D. N. Woolfson, *J. Mol. Biol.* **2009**, 385, 726-732.
[39] B. Apostolovic, M. Danial, H. A. Klok, *Chem. Soc. Rev.* **2010**, 39, 3541-3575.
[40] D. M. Raymond, B. L. Nilsson, *Chem. Soc. Rev.* **2018**, 47, 3659-3720.
[41] A. L. Boyle, D. N. Woolfson, *Chem. Soc. Rev.* **2011**, 40, 4295-4306.
[42] N. L. Ogihara, M. S. Weiss, D. Eisenberg, W. F. Degrado, *Protein Sci.* **1997**, 6, 80-88.
[43] L. Malik, J. Nygaard, N. J. Christensen, W. W. Streicher, P. W. Thulstrup, L. Arleth, K. J. Jensen, *J. Pept. Sci.* **2013**, 19, 283-292.

[44] B. Wlotzka, S. Leva, B. Eschgfäller, J. Burmeister, F. Kleinjung, C. Kaduk, P. Muhn, H. Hess-Stumpp, S. Klussmann, *Proc. Natl. Acad. Sci. U. S. A.* **2002**, 99, 8898-8902.
[45] N. C. Hauser, R. Martinez, A. Jacob, S. Rupp, J. D. Hoheisel, S. Matysiak, *Nucleic Acids Res.* **2006**, 34, 5101-5111.
[46] G E Plum, D S Pilch, a. S F Singleton, K. J. Breslauer, *Annu. Rev. Biophys. Biomol. Struct.* **1995**, 24, 319-350.
[47] M. Duca, P. Vekhoff, K. Oussedik, L. Halby, P. B. Arimondo, *Nucleic Acids Res.* **2008**, 36, 5123-5138.
[48] D. Schneidman-Duhovny, M. Hammel, J. A. Tainer, A. Sali, *Nucleic Acids Res.* **2016**, 44, W424-W429.

10.1002/chem.201905636

Entry for the Table of Contents

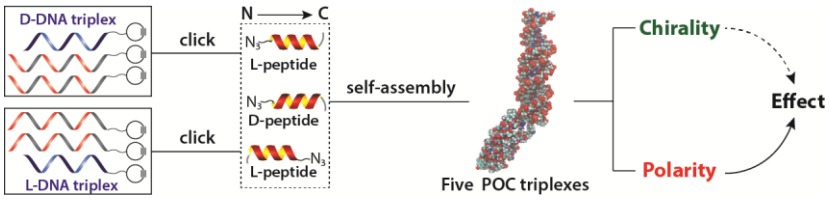

Artificial protein mimics: The self-assembly of five peptide coiled-coil motifs was templated by the hybridization of a D-DNA triplex or its mirror-image counterpart, an L-DNA triplex. The stabilizing cooperation between the two biomolecular domains was shown to be chirality-independent, but orientation-dependent.